ARTICLE
Journal of Cellular Biochemistry 105:885–895 (2008)

Journal of Cellular Biochemistry

Activating Transcription Factor 4 Is Critical for Proliferation and Survival in Primary Bone Marrow Stromal Cells and Calvarial Osteoblasts

Xiaoyan Zhang,[1,2] Shibing Yu,[1] Deborah L. Galson,[1] Min Luo,[1] Jie Fan,[3] Jian Zhang,[1] Youfei Guan,[2] and Guozhi Xiao[1*]

[1]*Department of Medicine, University of Pittsburgh, Pittsburgh, Pennsylvania 15240*

[2]*Department of Physiology and Pathophysiology, Peking (Beijing) University Health Science Center, Beijing 100083, China*

[3]*Department of Surgery, University of Pittsburgh, Pittsburgh, Pennsylvania 15240*

ABSTRACT

Activating transcription factor 4 (ATF4) is essential for bone formation. However, the mechanism of its actions in bone is poorly understood. The present study examined the role for ATF4 in the regulation of proliferation and survival of primary mouse bone marrow stromal cells (BMSCs) and osteoblasts. Results showed that *Atf4*$^{-/-}$ cells display a severe proliferative defect as measured by multiple cell proliferation assays. Cell cycle progression of *Atf4*$^{-/-}$ BMSCs was largely delayed with significant G1 arrest. Expression of cyclin D1 was decreased both at the mRNA and protein level. A similar proliferation defect was observed in *Atf4*$^{-/-}$ calvarial periosteal osteoblasts when compared with wt control. Knocking down *Atf4* mRNA by small interfering RNA in MC3T3-E1 subclone 4 preosteoblasts markedly reduced expression of cyclin D1 and cell proliferation. In contrast, overexpression of ATF4 increased cyclin D1 expression as well as cell proliferation in *Atf4*$^{-/-}$ BMSCs. In addition, apoptosis was significantly increased in *Atf4*$^{-/-}$ BMSCs and calvarial periosteal osteoblasts relative to wt controls. Taken together, these results for the first time demonstrate that ATF4 is a critical regulator of proliferation and survival in BMSCs and osteoblasts in vitro and in vivo. J. Cell. Biochem. 105: 885–895, 2008.

KEY WORDS: ATF4; OSTEOBLASTS; PROLIFERATION; APOPTOSIS; CELL CYCLE; CYCLIN D1

Activating transcription factor 4 (ATF4), also known as cAMP-response element-binding protein 2 (CREB2) [Karpinski et al., 1992] and Tax-responsive enhancer element B67 (TAXREB67) [Tsujimoto et al., 1991], is a ubiquitous basic leucine-zipper transcription factor that is a member of the ATF/CREB protein family. This family includes cAMP-response element-binding protein (CREB), cAMP-response element modulator (CREM), ATF1, ATF2, ATF3, and ATF4 [Ziff, 1990; Brindle and Montminy, 1992; Meyer and Habener, 1993; Sassone-Corsi, 1994; Hai et al., 1999]. ATF4 functions as both transcriptional repressor and activator by forming homodimers and heterodimers with members of the AP-1 and C/EBP family of protein, or interacting with many other partners, such as human T-cell lymphotropic virus type 1, granulocyte colony-stimulating factor promoter element 1-binding protein, insulin-like growth factor-binding protein-1, NF-E2-related factor 2, c-maf, p300, Zhangfei, factor inhibiting ATF4-mediated transcription, special AT-rich sequence binding protein 2, transcription factor IIAγ, and runt-related transcription factor 2 [Hai and Curran, 1991; Chevray and Nathans, 1992; Nishizawa and Nagata, 1992; Vallejo et al., 1993; Vinson et al., 1993; Motohashi et al., 1997; Reddy et al., 1997; He et al., 2001; Lassot et al., 2005; Xiao et al., 2005; Yu et al., 2005, 2008b; Dobreva et al., 2006; Hogan et al., 2006]. ATF4 expression is up-regulated by several factors/stressors, including oxygen deprivation, endoplasmic reticulum stress, oxidative stress [Ameri et al., 2004; Blais et al., 2004; Roybal et al., 2005].

Abbreviations used: ATF4, activating transcription factor 4; Foxo1, forkhead box O1; BMSCs, bone marrow stromal cells; CDKs, cyclin-dependent kinases; CDKIs, cyclin-dependent kinase inhibitors.

Grant sponsor: NIH; Grant number: DK072230; Grant sponsor: Department of Defense; Grant number: W81XWH-07-1-0160.

*Correspondence to: Dr. Guozhi Xiao, Rm 2E-109, VA Pittsburgh Healthcare System, 151-U, Pittsburgh, PA 15240. E-mail: xiaog@upmc.edu

Received 27 May 2008; Accepted 17 July 2008 • DOI 10.1002/jcb.21888 • 2008 Wiley-Liss, Inc.

Published online 26 August 2008 in Wiley InterScience (www.interscience.wiley.com).

A role for ATF4 in bone development was established using *Atf4*-deficient mice [Yang et al., 2004]. $Atf4^{-/-}$ mice have a dramatically reduced bone formation rate and bone mineral density (severe osteoporosis) that persists throughout life. The expression of both *osteocalcin* (*Ocn*) and *bone sialoprotein* (*Bsp*), both markers for terminally differentiated osteoblasts, was markedly reduced in *Atf4*-deficient osteoblasts, suggesting a critical role for ATF4 in osteoblast differentiation. The $Atf4^{-/-}$ skeleton is much smaller relative to its wild-type (wt) control littermate, suggesting reduced numbers of bone cells. However, it is not known if ATF4 regulates osteoblast proliferation.

Cell cycle progression is a complex process that regulates cell proliferation. Cell cycle consists of several phases including G1 (from the end of the previous M phase till the beginning of DNA synthesis), S (DNA synthesis), G2 (significant protein synthesis occurs during this phase), and M phase (cell splits itself into two distinct cells) [Sherr and Roberts, 2004]. In addition, quiescent cells are in G0 phase. Cell cycle progression is a highly regulated process in that DNA replication occurs only once in each cycle. Transition from one phase to another is regulated by distinct cyclin-dependent kinases (CDKs) that are regulated by various cyclins, CDK inhibitors, and phosphorylations. Distinct cyclins and appropriate CDKs form complexes that function at different points of the cell cycle [Sherr and Roberts, 2004]. For example, formation of cyclin D1-CDK4/6 complex in early to mid G1 phase activates the kinases that phosphorylate and inactivate the tumor suppressor Rb, a critical step that is necessary for the transition from G1 to S phase [Kato et al., 1994; Sherr, 1994; Zhao et al., 2001]. The activity of cyclin E-CDK2 is periodic and maximal at the G1 to S phase transition [Roberts et al., 1994; Ohtsubo et al., 1995]. Cyclin A1 activates CDK2 and is essential at the G1/S boundary and throughout S phase [Pagano et al., 1992]. In addition, cyclin-CDK complexes also have a noncatalytic role in G1 phase by sequestering proteins of the cip/kip family, including $p27^{kip}$ and $p21^{cip}$, both CDK2 inhibitors (CDKIs) that negatively regulate cell cycle progression [Hofmann and Livingston, 1996].

Apoptosis is a form of cell death in which a programmed sequence of events leads to the destruction of cells. It occurs in both physiological and pathological conditions when the body needs to eliminate aged cells, unnecessary cells, and unhealthy cells. The caspase family, a set of cysteine proteases that cleave a variety of substrates, plays a crucial role in apoptosis. Caspases are divided into two groups: ''initiator'' caspases such as caspase-8 and -9 and ''executioner'' caspases including caspase-3, -6, and -7 [Shi, 2002]. During apoptosis, after being activated by various forms of stress such as inadequate growth factor support and different types of intracellular damage, initiator caspases proteolytically cleave executioner caspases that cause cell death events such as cytoplasm shrinkage, chromatin condensation, and DNA fragmentation. B-cell lymphoma 2 (Bcl-2) is the prototype for a family of mammalian genes encoding the proteins that control mitochondrial outer membrane permeabilization (MOMP) and can be either pro-apoptotic (Bax, BAD, Bak, and Bok) or anti-apoptotic (including Bcl-2, Bcl-xL, and Bcl-w) [Adams, 2003]. $Atf4^{-/-}$ mice are blind due to excessive apoptosis of cells in the lens epithelium [Kato et al., 1994; Sherr and Roberts, 2004], suggesting a critical role for ATF4 in protecting these cells from apoptosis under physiological condition.

The aim of this study was to determine the effects of ATF4 in the regulation of proliferation and apoptosis in primary BMSCs and osteoblasts.

MATERIALS AND METHODS

REAGENTS

Tissue culture media were purchased from Invitrogen (Carlsbad, CA) and fetal bovine serum from HyClone (Logan, UT). Other reagents were obtained from the following sources: Antibodies against cyclins D1, D3, p21, p27, CDK2, and horseradish peroxidase-conjugated mouse or goat IgG from Santa Cruz (Santa Cruz, CA), mouse monoclonal antibody against β-actin from Sigma (St. Louis, MO), BrdU immunostaining kit (Zymed Laboratories Inc., San Francisco, CA) from Invitrogen, ApopTag Peroxidase In Situ Apoptosis Detection Kit from Chemicon (Temecula, CA). Hoechst staining reagent was kindly provided by Dr. Rentian Feng of the University of Pittsburgh. All other chemicals were of analytical grade.

Atf4–DEFICIENT MICE

Breeding pairs of ATF4 heterozygous mice were described previously [Yu et al., 2008a] and used to generate *Atf4* wild-type (wt) ($Atf4^{+/+}$), heterozygous ($Atf4^{+/-}$) and homozygous mutant ($Atf4^{-/-}$) mice for this study. All research protocols were approved by the Institutional Animal Care and Use Committee of the VA Pittsburgh Healthcare System, where this study was conducted.

HISTOLOGICAL EVALUATION

Six-week-old wt and $Atf4^{-/-}$ mice were euthanized and calvariae were fixed in 10% formalin at 4°C for 24 h, decalcified in 10% EDTA (pH 7.4) for 10 days, and embedded in paraffin. Calvariae were then bisected perpendicular to the sagittal suture through the central portion of the parietal bones, parallel to lamboidal and coronal sutures, and embedded in paraffin to obtain sections of a standard area according to the method described by Zhao et al. [2000].

CELL CULTURES AND ISOLATION OF PRIMARY BMSCs

Mouse MC3T3-E1 subclone 4 (MC-4) preosteoblasts were described previously [Xiao et al., 1997; Wang et al., 1999] and maintained in ascorbic acid-free alpha-modified Eagle's medium (alpha-MEM), 10% fetal bovine serum (FBS), and 1% penicillin/streptomycin (proliferation medium). Isolation of mouse primary BMSCs was described previously [Xiao et al., 2002]. Briefly, 6-week-old male wt and $Atf4^{-/-}$ mice were euthanized. Femurs and tibias were isolated and the epiphyses were cut. Marrow was flushed with alpha-MEM containing 20% FBS and 1% penicillin/streptomycin into a 100-mm dish and the cell suspension was aspirated up and down with a 20-gauge needle in order to break clumps of marrow. The cell suspension was then cultured in a T75 flask in the same medium. After 10 days, cells reached confluency and were ready for experiments.

ELECTROPORATION

Primary BMSCs were transfected using an Amaxa Nucleofector device (Cologne, Germany) as described by Nakashima et al. [2005]. Briefly, 2×10^6 BMSCs were suspended in 100 μl solution from Cell Line Nucleofector Kit V (Amaxa Biosystems, Cologne, Germany) and mixed with indicated plasmid DNAs. Cells were electroporated using the Program A-23 of the Amaxa Nucleofector device. Immediately after electroporation, cells were seeded for experiments.

MTS ASSAY

MTS assay was described previously [Singha et al., 2007]. Briefly, 1×10^4 cells/well were planted in a 96-well plate in 100 μl proliferation medium. Cells were incubated at 37°C for 24 h to allow attachment. The medium was changed every 48 h. At different time points, 20 μl of CellTitre96AQ solution reagent (Promega, Madison, WI) was added into each well and incubated for 2 h. Finally, the absorbance was recorded at 490 nm using a 96-well plate reader.

[^{3}H] THYMIDINE INCORPORATION

Cells were plated in 12-well plates at 5×10^4 cells/well in proliferation medium for 24 h and switched to 0.1% FBS alpha-MEM for another 24 h and [^{3}H] thymidine was then added to a final concentration of 5 μCi/ml and incubated at 37°C for 1 h in proliferation medium. Medium was removed by aspiration, and cells were washed twice with ice-cold serum-free alpha-MEM. Cell were extracted twice with 10% trichloroacetic acid (TCA) on ice for 5 min. TCA precipitates were solubilized by adding 10% SDS for 2 min at room temperature. Cells were harvested, and the amount of radioactivity was measured by liquid scintillation counting (Beckman Instruments, Inc., Fullerton, CA).

BROMODEOXYURIDINE (BrdU) INCORPORATION ASSAY

BrdU labeling reagent was purchased from Invitrogen. BrdU staining was performed using cells cultured in 8-well culture chambers (Nalgene Nunc, NY) or 10-μm sections of calvariae from wt and *Atf4*$^{-/-}$ mice. Cells were cultured in 8-well chamber at a density of 10^5 cells/well in 400 μl proliferation medium. After 4 days, cells from four identically treated wells per group were labeled with BrdU (1:100 dilution) overnight in the same medium. For calvarial sections, wt and *Atf4*$^{-/-}$ mice (6/group) were injected intraperitoneally with 100 μg bromodeoxyuridine (BrdU)/12 μg fluorodeoxyuridine (FdU) per gram of body weight 4 h before sacrifice. After sacrifice, 10-μm sections of calvariae were obtained as described previously [Demiralp et al., 2002]. To identify actively proliferating cells, nuclei that have incorporated BrdU were detected using a Zymed BrdU immunostaining kit according to the manufacturer's instruction. BrdU-positive cells on the periosteal surface of calvariae were counted and normalized to the total periosteal cell numbers in the same area [Zhao et al., 2004].

FLOW CYTOMETRIC ANALYSIS

Primary BMSCs from wt and *Atf4*$^{-/-}$ mice were cultured in proliferation medium for 4 days and harvested. 5×10^5 cells were suspended in 1 ml proliferation medium and Vybrant violent dye (Invitrogen) was added to a final concentration of 5 μM and incubated at 37°C for 30 min. The distribution of BMSCs throughout the cell cycle was assessed by flow cytometry using 405 nm excitation and 440 nm emission. The fraction of the population in each phase was determined as a function of DNA content using an FACS with software.

ApopTag PEROXIDASE IN SITU APOPTOSIS DETECTION

This method is based on the classical TUNEL assay to examine apoptosis by detecting DNA fragmentation. Primary BMSCs from wt and *Atf4*$^{-/-}$ mice were cultured in proliferation medium for 4 days and stained using the ApopTag Peroxidase In Situ Apoptosis Detection Kit according to the manufacturer's instruction. Cells were counterstained with Hematoxylin. Sections of wt and *Atf4*$^{-/-}$ calvariae (6/group) were prepared and stained using the same kit. Negative controls were made by omitting the terminal deoxynucleotidyl transferase (TdT). All positive (brown) and negative (blue) nuclei were counted. Apoptotic cells on the periosteal surface were counted and normalized to the total cells from the same area.

RNA ISOLATION AND REVERSE TRANSCRIPTION (RT)

Tibias (6/group) were isolated and soft tissues were removed. Tibias were frozen in liquid nitrogen and ground into powder using a mortar and pestle and total RNAs from each group were isolated using the Trizol reagent (Invitrogen) following the manufacturer's protocol. Reverse transcription (RT) was performed using 1 μg of denatured RNA and 100 pmol of random hexamers (Applied Biosystem, Foster, CA) in a total volume of 25 μl containing 12.5 U MultiScribe reverse transcriptase (Applied Biosystem).

QUANTITATIVE REAL-TIME PCR

Quantitative real-time PCR was performed on an iCycler (BIO-RAD, Minneapolis, MN) using a SYBR® Green PCR Core Kit (Applied Biosystem) and cDNA equivalent to 10 ng RNA in a 50 microliter reaction according to the manufacturer's instructions. The DNA sequences of mouse primers used for real-time PCR were: *cyclin D1* (GenBank Accession number-NM-007631), 5′ GAG GAG GGG GAA GTG GAG GA 3′ (forward, +1,049-bp), 5′ CCT CTT TGC GGG TGC CAC TA 3′ (reverse, +1,170-bp); *Foxo1*(GenBank Accession number-NM-019739), 5′ AGA GGC TCA CCC TGT CGC AGA 3′ (forward, +955-bp), 5′ GTG AAG GGA CAG ATT GTG GCG A 3′ (reverse, +1,080-bp); *Gapdh* (GenBank Accession number-NM-001001303), 5′-CAG TGC CAG CCT CGT CCC GTA GA-3′ (forward, +32-bp), 5′-CTG CAA ATG GCA GCC CTG GTG AC-3′ (reverse, +127-bp). For all primers the amplification was performed as follows: initial denaturation at 95°C for 10 min followed by 40 cycles of 95°C for 15 s and 60°C for 60 s. Melting curve analysis was used to confirm the specificity of the PCR products. Six samples were run for each primer set. The levels of mRNA were calculated by the ΔCT (the difference between the threshold cycles) method [Wang et al., 2004]. The mRNA level of each gene was normalized to *Gapdh* mRNA.

WESTERN BLOT ANALYSIS

Cells were washed with cold 1× PBS and lysed in 1× Passive Buffer (Promega) at RT for 20 min. Lysates were clarified by centrifugation (20 min, 13,000*g*, 4°C). For bone tissues, wt and *Atf4*$^{-/-}$ tibias (6/group) were frozen in liquid nitrogen and ground into powder

with a mortar and pestle. Samples were solubilized with 1× Passive Buffer for 20 min on ice and sonicated on ice (3 times, 5 s each) and lysates were then clarified by centrifugation (20 min, 13,000*g*, 4°C). Protein concentrations were determined by the method developed by Bio-Rad Laboratories, Inc. (Hercules, CA). Twenty-five microgram of total protein were fractionated on a 10% SDS–PAGE gel and transferred onto nitrocellulose membranes (Whatman). The membrane was blocked in 5% nonfat milk in Tris-buffered saline/Tween-20 (TBST) buffer, probed with antibodies (1:1,000) against cyclins D1, D3, CDK2, p21, and p27 followed by incubation with anti-rabbit or anti-mouse antibodies conjugated with horseradish peroxidase (1:5,000) and visualized using an enhanced chemiluminescence kit (Pierce, Rockford, IL). Finally, blots were striped 2 times in buffer containing 65 mM Tris–Cl (pH 6.8), 2% SDS, and 0.7% (v/v) β-mercaptoethanol at 65°C for 15 min and re-probed with β-actin antibody (1:2,000) for normalization.

SMALL INTERFERING RNA (siRNA)

MC-4 cells, which contain high levels of *Atf4* mRNA, were seeded at a density of 25,000 cells/cm^2. After 24 h, cells were transfected with mouse *Atf4* siRNA (sense: 5′-GAG CAU UCC UUU AGU UUA GUU-3′; antisense: 5′-CUA AAC UAA AGG AAU GCU CUU-3′) or negative control siRNA (low GC, Cat #: 12935-200, Invitrogen) [Adams, 2007; Yu et al., 2008a] using LipofectAMINE 2000 (Invitrogen). After 48 h, cells from three identically treated dishes were pooled and harvested for total RNA, followed by quantitative real-time RT-PCR analysis for *Atf4*, *cyclin D1* and *Foxo1* mRNAs. A second set of mouse *Atf4* siRNAs was purchased from Ambion (Cat #: AM16704, ID#: 160775 and 160776) and used to confirm the results using the first set of *Atf4* siRNA.

STATISTICAL ANALYSIS

Data was analyzed with GraphPad Prism software. Students' *t*-test was used to test for differences between two groups. A one-way ANOVA analysis was used followed by the Dunnett's test for Figures 1C, 5A–D, 6A–C, and 7A,B. Differences with a $P < 0.05$ were considered as statistically significant. All experiments were repeated a minimum of 3 times with triplicate samples.

RESULTS

ATF4 DEFICIENCY REDUCES CELL PROLIFERATION IN PRIMARY BMSCs and CALVARIAL PERIOSTEAL OSTEOBLASTS

To determine if ATF4 plays a role in the regulation of osteoblast proliferation, we performed several experiments. We first determined the effects of ATF4 deficiency on the numbers of total nucleated bone marrow cells, bone marrow from 6-week-old male wt and *Atf4*$^{-/-}$ mice (6/group) were isolated. After lysing the red blood cells (RBCs) using the RBC lysis buffer (Sigma), the remaining nucleated bone marrow cells were directly counted using a

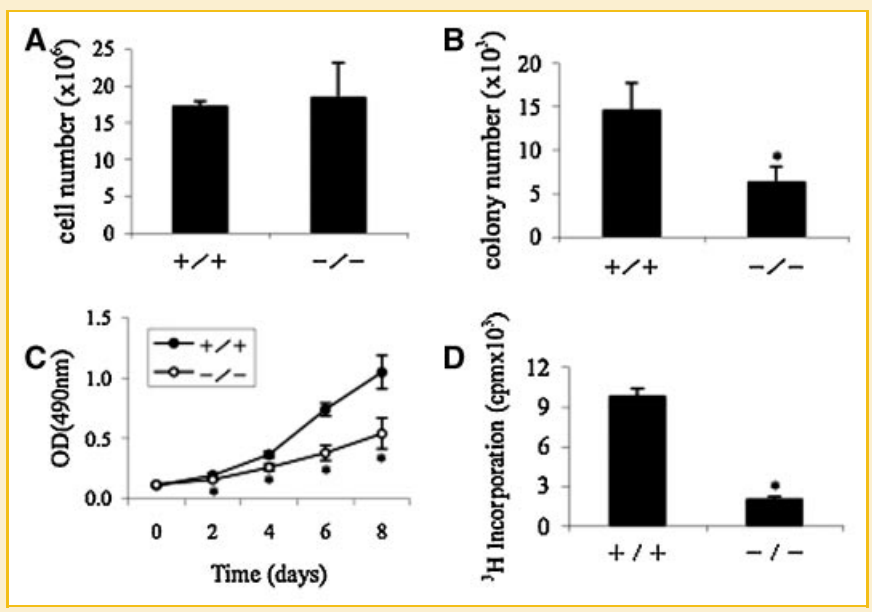

Fig. 1. ATF4 is required for primary BMSC proliferation. A: Total nucleated bone marrow cells. Long bones (two femurs and two tibias) from 6-week-old male wt and Atf4−/− mice (6 mice per group) were isolated. Bone marrow was flushed out and red blood cells (RBC) were lysed using the RBC lysis buffer. Total nucleated bone marrow cells were counted using a hemacytometer. B: Colony numbers in bone marrow. After lysing the RBCs, the remaining total nucleated bone marrow cells from each mouse (two femurs and two tibias, 6 mice/group) were diluted (1:2,000) and cultured in proliferation medium. 24 h later, the non-adhering cells were removed by washing the cells 3 times with 1× PBS. Cells were then cultured in proliferation medium for 10 days. The numbers of colonies were then counted using a microscope. C: MTS assay. Wt and *Atf4*$^{-/-}$ BMSCs were seeded at a density of 10^4 cells/well in 96-well plate and cultured in proliferation medium for 0, 2, 4, 6, and 8 days followed by incubation with 20 μl of CellTitre96AQ solution reagent for 2 h. The absorbance was recorded at 490 nm using a 96-well plate reader. D: [^{3}H] thymidine incorporation. wt and *Atf4*$^{-/-}$ BMSCs were plated in 12-well plates at 5×10^4 cells/well in proliferation medium for 24 h and switched to 0.1% FBS alpha-MEM for 24 h and [^{3}H] thymidine was then added to the culture (proliferation medium) to a final concentration of 5 μCi/ml and incubated at 37°C for 1 h. $^*P < 0.05$ (wt vs. *Atf4*$^{-/-}$), Data represent mean ± SD. Experiments were repeated 3 times and qualitatively identical results were obtained.

hemacytometer. As shown in Figure 1A, although the long bones of *Atf4*$^{-/-}$ mice were significantly shorter and thinner than those of wt mice, surprisingly, we found no significant difference in the numbers of total nucleated bone marrow cells between wt and *Atf4*$^{-/-}$ mice. This might be accounted by the relatively larger marrow cavity associated with the reduced cortical and trabecular bone volume observed in the *Atf4*$^{-/-}$ mice. We next determined whether ATF4 deficiency affects the numbers of total bone marrow stromal cells (BMSCs). After lysing the RBCs as described above, the remaining total nucleated bone marrow cells from each mouse (two femurs and two tibias, 6 mice/group) were diluted (1:2,000) and cultured in proliferation medium. Twenty-four hours later, the non-adhering cells were removed by washing the cells 3 times with 1× PBS. Cells were then cultured in proliferation medium for 10 days. The numbers of colonies from each dish were then counted using a microscope. As shown in Figure 1B, the number of BMSC colonies per mouse (from two femurs and two tibias) was significantly reduced in *Atf4*$^{-/-}$ group compared to values in the wt group ($P < 0.05$, wt vs. *Atf4*$^{-/-}$). This decrease could be explained by a cell-autonomous defect in proliferation and/or survival or could be secondary to an impaired bone microenvironment due to ATF4 deficiency. To differentiate these possibilities, we conducted MTS and [^{3}H] thymidine incorporation assays. For the MTS assay, 10^4 cells/well of wt and *Atf4*$^{-/-}$ BMSCs were seeded in 96-well plate and were cultured in proliferation medium for 0, 2, 4, 6, and 8 days. Cell numbers were then measured as described previously [Singha et al., 2007]. As shown in Figure 1C, ATF4-deficient cells grew at significantly reduced rates compared to wt cells. For the [^{3}H] thymidine incorporation assays, wt and *Atf4*$^{-/-}$ BMSCs were cultured in proliferation medium for 4 days and labeled with [^{3}H] thymidine for 1 h before harvesting. As shown in Figure 1D, [^{3}H] thymidine incorporation into the DNA of *Atf4*$^{-/-}$ BMSCs was decreased by fourfold compared to values in wt cells ($P < 0.05$, wt vs. *Atf4*$^{-/-}$). It should be noted that the adherent murine BMSC population is contaminated with macrophages, however, macrophages and their precursors would be less proliferative under the culture conditions used, consequently, the proliferation measured is primarily that of BMSCs. To determine if ATF4 is required for osteoblast proliferation in vivo, 6-week-old wt and *Atf4*$^{-/-}$ mice were injected with bromodeoxyuridine (BrdU)/fluorodeoxyuridine (FdU) 4 h before sacrifice, 10-μm sections of calvariae were obtained, and proliferating cells from the periosteal surface were counted and normalized to total cells from the same area. As shown in Figure 2A, in wt calvariae, periosteal osteoblasts proliferated very actively with 60% of the total cells being BrdU-positive. In contrast, the percent BrdU-positive osteoblasts were significantly reduced in *Atf4*$^{-/-}$ calvariae ($P < 0.05$, wt vs. *Atf4*$^{-/-}$) (Fig. 2B,C). It should be noted that very few osteocytes (mature osteoblasts) that permeate the bone matrix were stained BrdU-positive in both wt and *Atf4*$^{-/-}$ calvariae. Thus, ATF4 is required for the proliferation of BMSCs or osteoblasts both in vitro and in vivo.

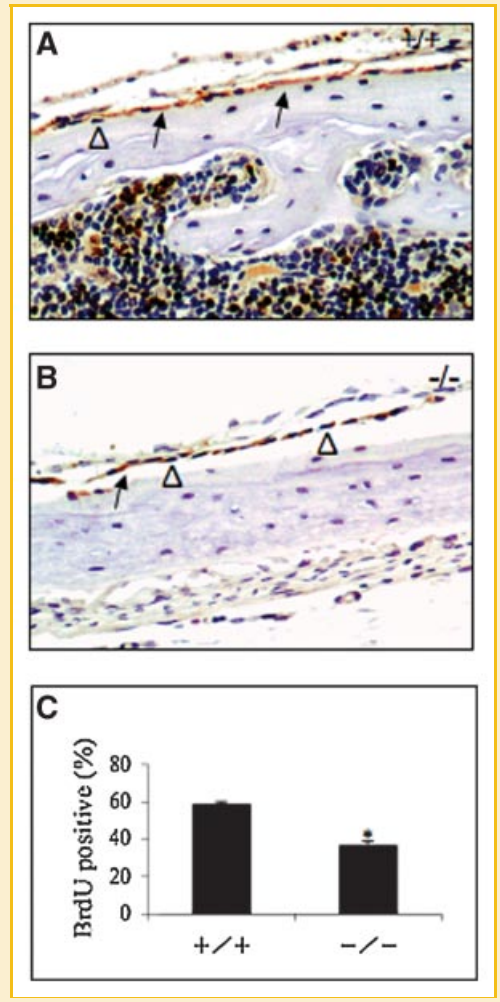

Fig. 2. ATF4 is required for proliferation of calvarial periosteal osteoblasts in vivo. Six-week-old male wt (A) and *Atf4*$^{-/-}$ (B) mice (6 mice per group) were injected intraperitoneally with 100 μg bromodeoxyuridine (BrdU)/12 μg fluorodeoxyuridine (FdU) per gram of body weight 4 h before sacrifice. After sacrifice, sections of calvariae were obtained. C: BrdU positive cells on the periosteal surface of calvariae were counted and normalized to the total cells from the same area. $^*P < 0.05$ (wt vs. *Atf4*$^{-/-}$). Data represent mean ± SD. Arrows indicate BrdU-positive (proliferating) cells and Δ indicates BrdU-negative (nonproliferating) cells. [Color figure can be viewed in the online issue, which is available at www.interscience.wiley.com.]

ATF4 IS REQUIRED FOR CELL CYCLE PROGRESSION AND CYCLIN D1 EXPRESSION

To determine whether ATF4 is required for cell cycle progression, we performed flow cytometric analysis to compare the cell distribution across different phases of the cell cycle between wt and *Atf4*$^{-/-}$ BMSCs. As shown in Figure 3, ATF4-deficient cells showed a significant decrease in the cell distribution into both S and G2/M phases (32% and 45% change, respectively) when compared with values of wt control cells ($P < 0.05$, wt vs. *Atf4*$^{-/-}$). In contrast, the fraction of the cells in G1 was not reduced by ATF4 deficiency ($P > 0.05$, wt vs. *Atf4*$^{-/-}$). Cell-cycle progression from one phase to another is controlled by cyclin-dependent kinases (CDKs) whose activity is mainly regulated by distinct cyclins and cyclin-dependent kinase inhibitors (CDKIs). We examined the effects of ATF4 deficiency on the expression levels of critical cyclin D1, a major regulator of cell cycle progression and cell proliferation, and CDKIs. Wt and *Atf4*$^{-/-}$ BMSCs were cultured in proliferation medium for

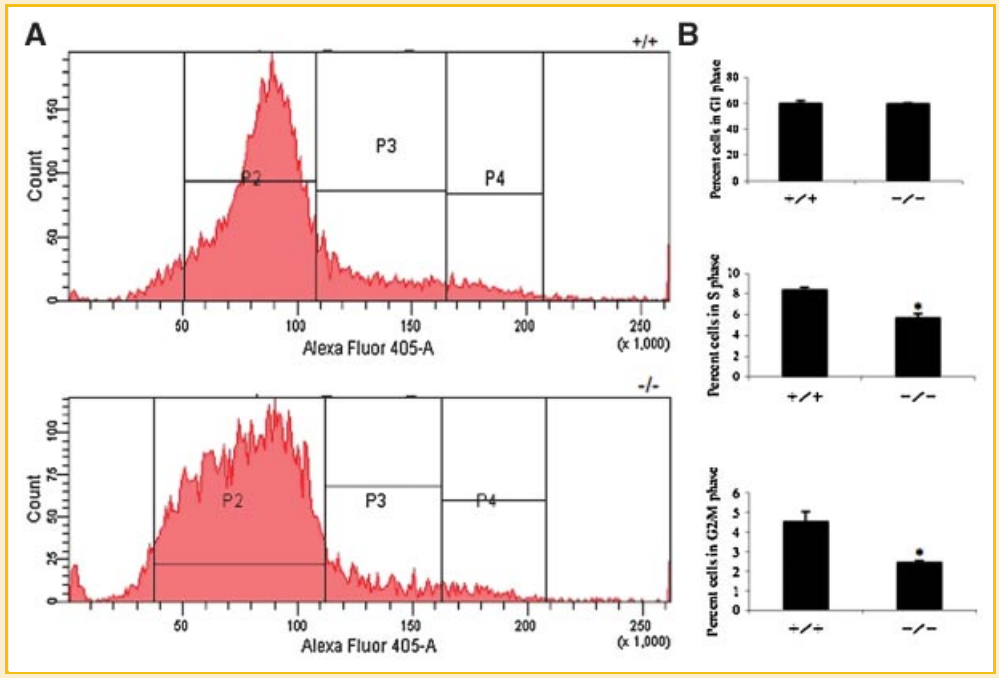

Fig. 3. ATF4 deficiency attenuates cell cycle progression. 5×10^5 wt (A, top) and Atf4−/− (A, bottom) BMSCs were suspended in 1.0 ml proliferation medium and labeled using the Vybrant DyeCycle Violet Stain Kit according to the manufacturer's instruction (Invitrogen). Cell population of different cell cycle phases was then measured by flow cytometry using 405 nm excitation and 440 nm emission. Quantitative data are presented in panel B. $^*P < 0.05$ (wt vs. *Atf4*$^{-/-}$). Data represent mean ± SD. Experiments were repeated 3 times and qualitatively identical results were obtained. P2, P3, and P4 represent cell population of G1, S and G2/M phases, respectively. It should be noted that scales are different from +/+ and −/−. [Color figure can be viewed in the online issue, which is available at www.interscience.wiley.com.]

4 days followed by Western blot analysis for cyclin D1, CDK2, p21, and p27. As shown in Figure 4A, the protein level of cyclin D1 was markedly decreased in *Atf4*$^{-/-}$ cells relative to wt control. In contrast, the level of p21 protein was slightly increased in *Atf4*$^{-/-}$ cells. Levels of both p27 and CDK2 proteins were low in BMSCs and their relative abundance did not display any significant difference between wt and *Atf4*$^{-/-}$ cells. Quantitative real-time RT/PCR analysis shows that the level of *cyclin D1* mRNA was reduced by 52% in *Atf4*$^{-/-}$ cells compared to values in wt controls ($P < 0.05$, wt vs. *Atf4*$^{-/-}$) (Fig. 4B). Note: as expected, minimal *Atf4* mRNA was detected by real-time RT/PCR in *Atf4*$^{-/-}$ cells (Fig. 4B, top).

To determine whether ATF4 is required for proliferation of the pre-osteoblast cell line, MC-4, which expresses high levels of *Atf4* mRNA and protein, the cells were transiently transfected with the indicated concentrations of *Atf4* siRNA or negative control siRNA (Invitrogen). This siRNA specifically targets mouse *Atf4* mRNA [Adams, 2007; Yu et al., 2008a]. As shown in Figure 5A, levels of *Atf4* mRNA were efficiently reduced by *Atf4* siRNA in a dose-dependent manner. In contrast, the negative control (40 nM) did not reduce *Atf4* mRNA. Importantly, the level of *cyclin D1* mRNA was significantly reduced by *Atf4* siRNA in a dose-dependent manner (Fig. 5B). Conversely, the level of *Foxo1* mRNA, a factor of the forkhead transcription factor family, was not reduced by *Atf4* siRNA (Fig. 5C). Furthermore, knocking-down *Atf4* mRNA markedly reduced MC-4 proliferation as measured by both MTS (Fig. 5D) and BrdU incorporation assays (Fig. 5E–G) ($P < 0.05$, ctrl siRNA vs. *Atf4* siRNA). Similar results were obtained when a different set of *Atf4* siRNAs was used in MC-4 cells (data not shown).

OVEREXPRESSING ATF4 RESCUES THE DEFECT IN CELL PROLIFERATION IN *Atf4*$^{-/-}$ BMSCs

We next determined whether overexpression of ATF4 could increase cell proliferation in BMSCs. To this end, we used a Cell Line

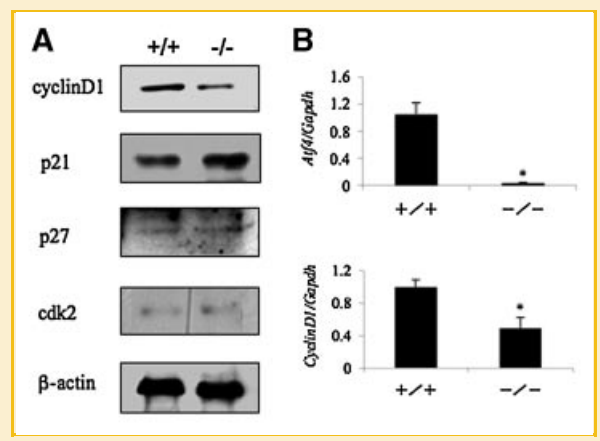

Fig. 4. ATF4 deficiency decreases cyclins D1 expression in primary BMSCs. A: Western blot analysis. wt and *Atf4*$^{-/-}$ BMSCs were seeded at a density of 5×10^4 cells/cm^2 in 35-mm dish and cultured in proliferation medium for 4 days. Whole cell extracts were used for Western blot analysis for cyclin D1, p21, p27, CDK2, and beta-actin (for loading). B: Quantitative real-time RT/PCR. wt and *Atf4*$^{-/-}$ BMSCs were treated as in (A) and harvested for RNA isolation and quantitative real-time RT/PCR analysis for cyclin D1 and Atf4 mRNAs that were normalized to Gapdh mRNA. $^*P < 0.05$ (wt vs. *Atf4*$^{-/-}$). Experiments were repeated 3 times and qualitatively identical results were obtained.

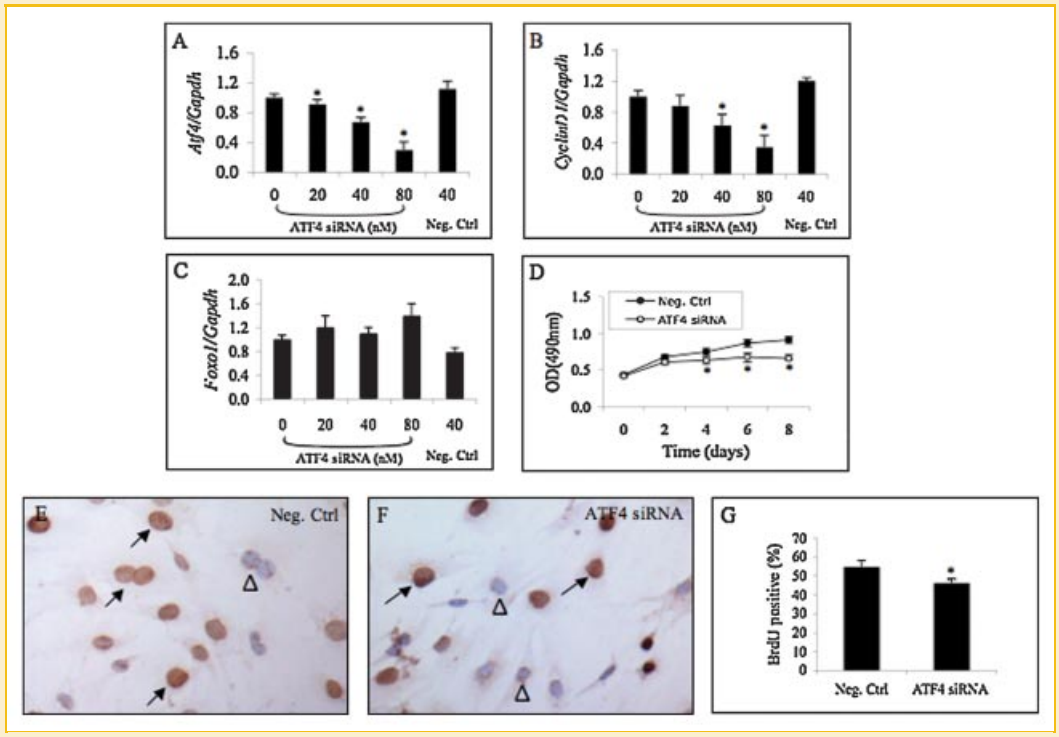

Fig. 5. ATF4 siRNA blocks endogenous cyclin D1 expression and inhibits cell proliferation in MC-4 Cells. A–C: Quantitative real-time RT/PCR. MC-4 cells were seeded at a density of 5×10^4 cells/cm^2 in 35-mm dish and transiently transfected with ATF4 siRNA (0, 20, 40, 80 nM) or negative control siRNA (40 nM). After 48 h, total RNA was prepared for quantitative real-time RT-PCR analysis for Atf4, cyclin D1 and Foxo1 mRNAs that were normalized to Gapdh mRNA. D: MTS assay. MC-4 cells were first seeded at a density of 5×10^4 cells/cm^2 in 100-mm dish and transiently transfected with 40 nM ATF4 siRNA or negative control siRNA. After 24 h, cells were re-seeded at 10^4 cells/well in 96-well plate in proliferation medium for indicated times followed by MTS assay. E–G: BrdU staining. MC-4 cells were seeded at 10^5 cells/well in 8-well chamber and transiently transfected with 40 nM ATF4 siRNA or negative control siRNA and cultured in proliferation medium for 4 days followed by BrdU staining. $^*P < 0.05$ (control siRNA vs. ATF4 siRNA). Data represent mean $\pm$ SD. Experiments were repeated at least 3 times and qualitatively identical results were obtained. Arrows indicate BrdU-positive (proliferating) cells and Δ indicates BrdU-negative (non-proliferating) cells. [Color figure can be viewed in the online issue, which is available at www.interscience.wiley.com.]

Nucleofector Kit V and a Nucleofector Device from Amaxa Biosystem (Cologne, Germany) because primary mouse BMSCs were transfected with higher than 40% efficiency by using this method (data not shown). To determine the effects of ATF4 overexpression on cyclins expression, *Atf4*$^{-/-}$ BMSCs were electroporated with increasing amounts of FLAG-ATF4-YFP expression vector (0, 0.5, 1, and 2 μg) [Xiao et al., 2005]. Thirty hours later, cells were harvested for the preparation of total RNA or protein. In addition, as shown in Figure 6A, *Atf4* mRNA was efficiently expressed in primary BMSCs in a dose-dependent manner. As shown in Figure 6B,D, ATF4 dose-dependently stimulated cyclin D1 expression both at the mRNA and protein level. In contrast, overexpressing ATF4 failed to elevate the level of cyclin D3 mRNA and protein (Fig. 6C,D). As shown in Figure 7, ATF4 overexpression significantly increased the rate of proliferation in *Atf4*$^{-/-}$ BMSC as measured by direct cell count, MTS assay, and BrdU staining ($P < 0.05$, ctrl vs. ATF4). Overexpressing ATF4 similarly increased cyclin D1 expression and cell proliferation in wt BMSCs (data not shown).

Taken together, these results clearly establish that ATF4 increases cell proliferation probably via promoting expression of cyclin D1 and cell cycle progression.

ATF4 DEFICIENCY INCREASES CELL APOPTOSIS

ATF4 is known to prevent lens epithelium from apoptosis [Tanaka et al., 1998; Hettmann et al., 2000]. As an initial step to determine if ATF4 regulates apoptosis in BMSCs, wt and *Atf4*$^{-/-}$ cells were cultured in proliferation media for 4 days and stained by the Hoechst method [Yamanaka et al., 2003]. As shown in Figure 8A–C, the numbers of apoptotic cells including those with shrinking cytoplasm and chromatin condensation (early apoptosis) and DNA fragmentation (late apoptosis) were increased greater than fivefold in *Atf4*$^{-/-}$ BMSCs compared to wt cells ($P < 0.05$, wt vs. *Atf4*$^{-/-}$). To confirm this finding, wt and *Atf4*$^{-/-}$ BMSCs were stained using the ApopTag Peroxidase In Situ Apoptosis Detection Kit, a modified TUNEL staining that measures DNA fragmentation in situ. As shown in Figure 8D–F, the percent apoptotic cells in *Atf4*$^{-/-}$ BMSCs were increased by 1.6-fold when compared to wt cells ($P < 0.05$, wt vs. *Atf4*$^{-/-}$). To determine if ATF4 deficiency increases osteoblast apoptosis in vivo, 10-μm calvarial sections from wt and *Atf4*$^{-/-}$ mice were obtained and stained using the same kit. Apoptotic cells that stained brown on the periosteal surface of calvariae were counted and normalized to total cells of the same periosteal surface. As shown in Figure 8G–I, a significant increase in apoptosis was found in *Atf4*$^{-/-}$ mice compared to wt controls ($P < 0.05$, wt vs.

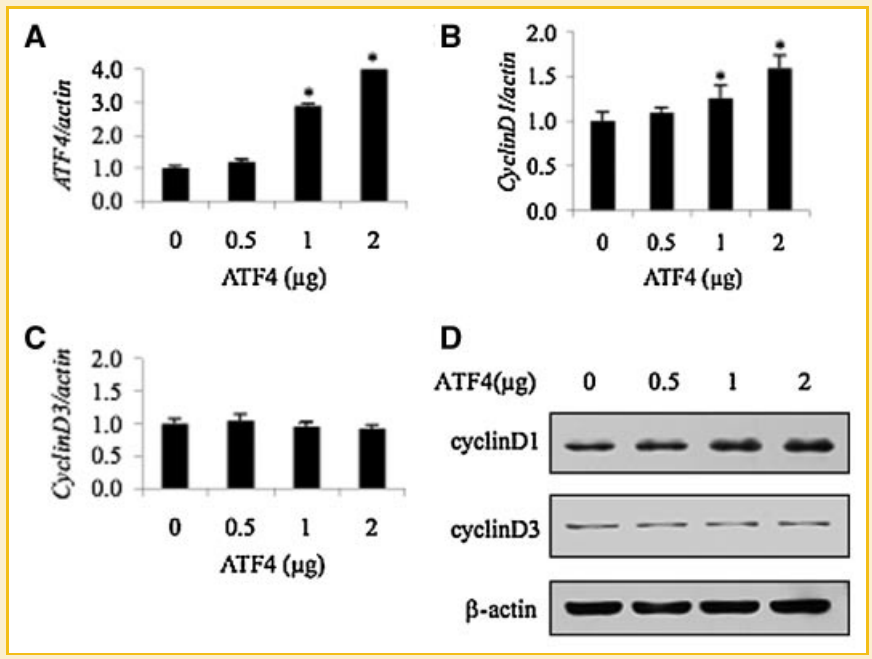

Fig. 6. Overexpression of ATF4 increases cyclin D1 expression. A–C: Quantitative real-time-RT/PCR. *Atf4*$^{-/-}$ BMSCs (2×10^6 cells/group) were electroporated with increasing amounts of FLAG-ATF4-YFP expression vector (0, 0.5, 1, and 2 μg). The amount of plasmid DNAs was balanced as necessary with beta-galactosidase expression plasmid such that the total DNA was constant in each group. Thirty hours later, cells were harvested for the preparation of total RNA and quantitative real-time RT/PCR analysis. D: Western blot analysis. Cells were treated as in (A) and harvested for whole cell extracts preparation and Western blot analysis. $^*P < 0.05$ (beta-gal vs. ATF4). Data represent mean ± SD. Experiments were repeated at least 3 times and qualitatively identical results were obtained.

Atf4$^{-/-}$). Thus, ATF4 protects osteoblasts from apoptosis under physiological condition.

DISCUSSION

In this study, we used two complementary approaches to establish the requirement for ATF4 in the regulation of proliferation in primary BMSCs and a preosteoblast cell line (MC-4 cells): (i) loss-of-function studies using *Atf4*$^{-/-}$ or *Atf4* siRNA-treated cells demonstrate that cell proliferation is significantly reduced in the absence of ATF4; and (ii) gain-of-function experiments via overexpression of ATF4 show that ATF4 enhances osteoblast proliferation in both wt and *Atf4*$^{-/-}$ BMSCs. In addition, this study reveals that ATF4 protects osteoblasts against apoptosis. Thus, the reduced bone mass

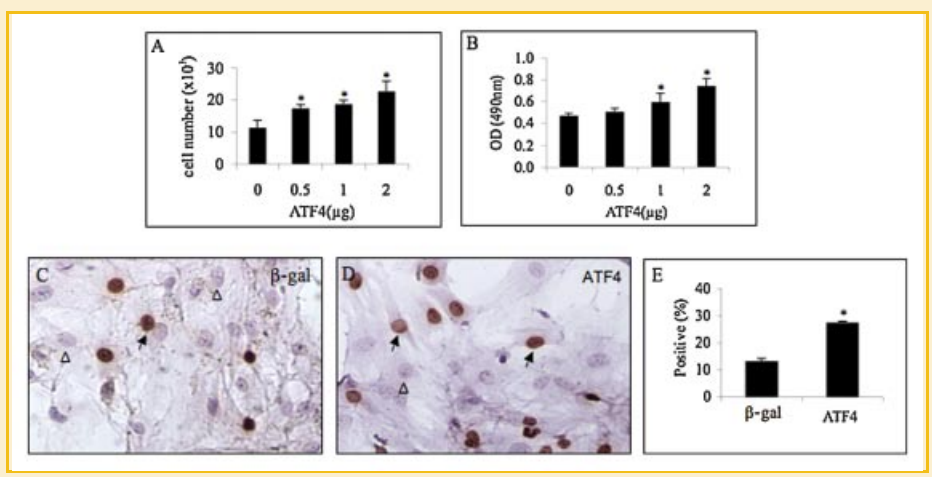

Fig. 7. Overexpression of ATF4 increases BMSC proliferation. A: Direct cell count. *Atf4*$^{-/-}$ BMSCs were electroporated as in Figure 6A. 5×10^3 cells/well were seeded in 96-well plates in proliferation medium for 4 days followed by direct cell count using a hemacytometer. B: MTS assay. Cells were electroporated as in Figure 6A. After electroporation, cells were used for the MTS assay as in Figure 1C. C–E: BrdU staining. Cells were electroporated as in Figure 6A. After electroporation, cells were used for the BrdU staining. $^*P < 0.05$ (beta-gal vs. ATF4). Data represent mean ± SD. Experiments were repeated at least 3 times and qualitatively identical results were obtained. Arrows indicate BrdU-positive (proliferating) cells and Δ indicates BrdU-negative (nonproliferating) cells. [Color figure can be viewed in the online issue, which is available at www.interscience.wiley.com.]

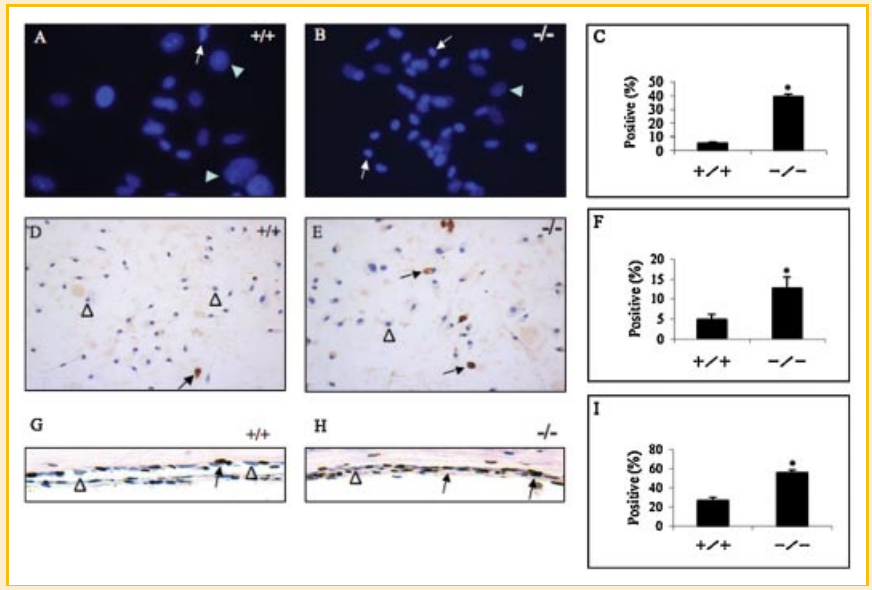

Fig. 8. ATF4 deficiency increases apoptosis in osteoblasts. A–C: Hoechst staining. wt and *Atf4*$^{-/-}$ BMSCs were seeded at a density of 5×10^4 cells/cm^2 in 35-mm dishes, cultured in proliferation medium for 4 days, and incubated with 1 μl of Hoechst dye at 37°C for 30 min. Cell images were obtained under UV light using a microscope (Olympus IX70). D–F: Apoptosis assay in BMSCs. wt and *Atf4*$^{-/-}$ BMSCs were seeded at 10^5 cells/well in 8-well chamber, cultured in proliferation medium for 4 days, and stained using the ApopTag Peroxidase In Situ Apoptosis Detection Kit according the manufacturer's instruction. G–I: Apoptosis assay in calvarial sections. Sections of calvariae from 6-week-old male wt and *Atf4*$^{-/-}$ mice (6 mice per group) were stained using the same kit. $P < 0.05$ (wt vs. *Atf4*$^{-/-}$). Data represent mean ± SD. Arrows indicate apoptotic cells and indicates nonapoptotic cells. [Color figure can be viewed in the online issue, which is available at www.interscience.wiley.com.]

and bone mineral density observed in ATF4 knock-out mice could be at least in part caused by decreased proliferation and increased apoptosis of *Atf4*$^{-/-}$ osteoprogenitors and osteoblasts.

While our results clearly show that the proliferation rate was significantly decreased in *Atf4*$^{-/-}$ BMSCs or *Atf4* siRNA-treated MC-4 cells (Figs. 1C and 5D), the magnitude of inhibition of cell proliferation by *Atf4* siRNA in MC-4 cells was markedly lower compared to that in *Atf4*$^{-/-}$ BMSCs. This discrepancy is likely due to our observation that the control siRNA treatment of MC-4 cells non-specifically reduces cell proliferation, which could mask the inhibitory effect of the *Atf4* siRNA on cell proliferation. In addition, the *Atf4* siRNA may not completely knock down the *Atf4* mRNA in MC-4 cells.

Previous studies established that ATF4 is critical for osteoblast differentiation as demonstrated by dramatically reduced expression of *osteocalcin* and *bone sialoprotein* mRNA in ATF4-deficient mice [Yang et al., 2004]. The present study demonstrates an essential role for ATF4 in the regulation of BMSC and osteoblast proliferation. *Atf4*$^{-/-}$ BMSCs and osteoblasts proliferate at a dramatically reduced rate compared to wt cells both in vitro and in vivo. Overexpressing ATF4 in *Atf4*$^{-/-}$ BMSCs rescues the proliferative defect. Expression of cyclin D1 is highly dependent upon the presence of ATF4 as demonstrated by the dramatic reduction in its mRNA and protein in *Atf4*$^{-/-}$ BMSCs. Reduced expression of cyclin D1 and possibly other cyclins in *Atf4*$^{-/-}$ cells leads to a lack of progression from G1 into the S and G2/M phases of the cell cycle. Since the percentage of the population in G1 is not affected by ATF4 deficiency, there must be concomitantly an increase in the percentage of G0 cells (quiescent cells) and/or cells undergoing cell death, thereby reducing overall cell proliferation.

Cyclin D1 is a key sensor and integrator of extracellular signals of cells and plays a critical role in cell cycle progression and proliferation [Stacey, 2003]. The expression level of cyclin D1 has been shown to be rate-limiting in cell proliferation induced by a variety of stimuli [Zhao et al., 2001]. Our results show that ATF4 is a key regulator of cyclin D1 expression in BMSCs or osteoblasts. Levels of cyclin D1 mRNA and protein are significantly reduced in the absence of ATF4. Forced expression of ATF4 efficiently augmented the level of *cyclin D1* mRNA as well as cell proliferation in both wt and *Atf4*$^{-/-}$ cells. Mechanisms whereby ATF4 increases *cyclin D1 mRNA* remain to be determined. An ATF/CRE site located in the proximal region of *cyclin D1* promoter was reported to bind to CREB and AP1 proteins and mediate active transcription of the gene [Sabbah et al., 1999; Nagata et al., 2001; Datta et al., 2007]. It is likely that ATF4 directly binds to this ATF/CRE site and activates transcription. It is also probable that ATF4 activates the *cyclin D1* promoter through interactions with CREB and AP1 proteins. Finally, ATF4 can stabilize *cyclin D1* mRNA through post-transcriptional mechanisms. Future study will differentiate these possibilities.

The periosteal surface of calvariae is mainly occupied by four cell types: osteoblasts or osteoprogenitors, bone lining cells, and osteoclasts. In rapidly growing animals, osteoblasts or osteoprogenitors are the major cells that cover the surface. In contrast, bone lining cells occupy the majority of the surface in adult or aged bones that have reached peak bone mass. Calvaria, which does not involve endochondral bone formation, has a relatively simple structure relative to other bones such as long bones and vertebrae. In addition, it is easy to histologically localize the osteoprogenitors/osteoblasts on the periosteal surface of calvaria. Therefore, it provides a unique model system for studying the functions of osteoblasts in vivo.

Using this model system, we found that osteoblasts from wt 6-week-old mice proliferate very actively on the periosteal surface (Fig. 2A). Conversely, proliferation of $Atf4^{-/-}$ osteoblasts is significantly reduced (Fig. 2B,C). Thus, an in vivo role for ATF4 in osteoblast proliferation is established. In support of our findings, Masuoka and Townes [2002] showed that $Atf4^{-/-}$ mice have severe fetal anemia due to impaired fetal-liver definitive hematopoiesis associated with a proliferative defect in fetal-liver cells. Furthermore, primary murine embryonic fibroblasts (MEFs) from $Atf4^{-/-}$ mice also display a defect in proliferation [Masuoka and Townes, 2002]. Lastly, transgenic overexpression of ATF4 in the developing lens results in hyperproliferation of lens fiber cells [Hettmann et al., 2000]. These results suggest that ATF4 is critical for proliferation of rapidly growing cells (i.e., BMSCs, osteoblasts, fetal-liver cells, MEFs, and lens fiber cells). Consistent with this notion, ATF4 is usually expressed at high level in rapidly growing tissues or cells [Tanaka et al., 1998; Hettmann et al., 2000; Masuoka and Townes, 2002; Yang et al., 2004].

The numbers of osteoblasts are eventually determined by the relative rate of cell proliferation and death by apoptosis. Experiments from this study establish that ATF4 is anti-apoptotic in BMSCs and osteoblasts. Nevertheless, ATF4 is not a global anti-apoptotic factor since no increase in apoptosis has been observed in $Atf4^{-/-}$ fetal liver cells although the ability of these cells to proliferate is impaired. ATF4 may elicit its anti-apoptotic function in combination with other factors in specific tissue and cells types. Thus, ATF4 deficiency increases apoptosis in lens fiber cells in a p53-dependent manner. The embryonic lens in double homozygous $p53/Atf4^{-/-}$ mice does not undergo apoptosis [Tanaka et al., 1998; Hettmann et al., 2000]. Interestingly, ATF4 expression is usually induced by oxygen deprivation, endoplasmic reticulum stress, and the oxidative stressor arsenite, all of which are known to induce cell apoptosis [Ameri et al., 2004; Blais et al., 2004; Roybal et al., 2005]. Therefore, it is reasonable to speculate that expression of ATF4 induced by apoptosis-inducing factors in fact provides a protection mechanism for cells to antagonize apoptosis. The molecular mechanism whereby ATF4 regulates apoptosis in osteoblasts remains to be determined in future study.

In summary, this study for the first time establishes that ATF4 is essential for cell proliferation and anti-apoptosis in BMSCs and osteoblasts.

ACKNOWLEDGMENTS

Thanks to Diane George and Dr. Scott Kulich of the VA Pittsburgh Healthcare System for assistance in bone histology and the Nucleofector electroporation transfection, respectively. This work was supported by an NIH Grant DK072230 and a Department of Defense Grant W81XWH-07-1-0160 (to G.X.) and two China National Natural Science Foundation grants NNSF 30530340 and NNSF 30725033 (to Y.G).

REFERENCES

Adams JM. 2003. Ways of dying: Multiple pathways to apoptosis. Genes Dev 17:2481–2495.

Adams CM. 2007. Role of the transcription factor ATF4 in the anabolic actions of insulin and the anti-anabolic actions of glucocorticoids. J Biol Chem 282:16744–16753.

Ameri K, Lewis CE, Raida M, Sowter H, Hai T, Harris AL. 2004. Anoxic induction of ATF-4 through HIF-1-independent pathways of protein stabilization in human cancer cells. Blood 103:1876–1882.

Blais JD, Filipenko V, Bi M, Harding HP, Ron D, Koumenis C, Wouters BG, Bell JC. 2004. Activating transcription factor 4 is translationally regulated by hypoxic stress. Mol Cell Biol 24:7469–7482.

Brindle PK, Montminy MR. 1992. The CREB family of transcription activators. Curr Opin Genet Dev 2:199–204.

Chevray PM, Nathans D. 1992. Protein interaction cloning in yeast: Identification of mammalian proteins that react with the leucine zipper of Jun. Proc Natl Acad Sci USA 89:5789–5793.

Datta NS, Pettway GJ, Chen C, Koh AJ, McCauley LK. 2007. Cyclin D1 as a target for the proliferative effects of PTH and PTHrP in early osteoblastic cells. J Bone Miner Res 22:951–964.

Demiralp B, Chen HL, Koh AJ, Keller ET, McCauley LK. 2002. Anabolic actions of parathyroid hormone during bone growth are dependent on c-fos. Endocrinology 143:4038–4047.

Dobreva G, Chahrour M, Dautzenberg M, Chirivella L, Kanzler B, Farinas I, Karsenty G, Grosschedl R. 2006. SATB2 is a multifunctional determinant of craniofacial patterning and osteoblast differentiation. Cell 125:971–986.

Hai T, Curran T. 1991. Cross-family dimerization of transcription factors Fos/Jun and ATF/CREB alters DNA binding specificity. Proc Natl Acad Sci USA 88:3720–3724.

Hai T, Wolfgang CD, Marsee DK, Allen AE, Sivaprasad U. 1999. ATF3 and stress responses. Gene Expr 7:321–335.

He CH, Gong P, Hu B, Stewart D, Choi ME, Choi AM, Alam J. 2001. Identification of activating transcription factor 4 (ATF4) as an Nrf2-interacting protein. Implication for heme oxygenase-1 gene regulation. J Biol Chem 276:20858–20865.

Hettmann T, Barton K, Leiden JM. 2000. Microphthalmia due to p53-mediated apoptosis of anterior lens epithelial cells in mice lacking the CREB-2 transcription factor. Dev Biol 222:110–123.

Hofmann F, Livingston DM. 1996. Differential effects of cdk2 and cdk3 on the control of pRb and E2F function during G1 exit. Genes Dev 10:851–861.

Hogan MR, Cockram GP, Lu R. 2006. Cooperative interaction of Zhangfei and ATF4 in transactivation of the cyclic AMP response element. FEBS Lett 580:58–62.

Karpinski BA, Morle GD, Huggenvik J, Uhler MD, Leiden JM. 1992. Molecular cloning of human CREB-2: An ATF/CREB transcription factor that can negatively regulate transcription from the cAMP response element. Proc Natl Acad Sci USA 89:4820–4824.

Kato JY, Matsuoka M, Polyak K, Massague J, Sherr CJ. 1994. Cyclic AMP-induced G1 phase arrest mediated by an inhibitor (p27Kip1) of cyclin-dependent kinase 4 activation. Cell 79:487–496.

Lassot I, Estrabaud E, Emiliani S, Benkirane M, Benarous R, Margottin-Goguet F. 2005. p300 modulates ATF4 stability and transcriptional activity independently of its acetyltransferase domain. J Biol Chem 280:41537–41545.

Masuoka HC, Townes TM. 2002. Targeted disruption of the activating transcription factor 4 gene results in severe fetal anemia in mice. Blood 99:736–745.

Meyer TE, Habener JF. 1993. Cyclic adenosine 3′,5′-monophosphate response element binding protein (CREB) and related transcription-activating deoxyribonucleic acid-binding proteins. Endocr Rev 14:269–290.

Motohashi H, Shavit JA, Igarashi K, Yamamoto M, Engel JD. 1997. The world according to Maf. Nucleic Acids Res 25:2953–2959.

Nagata D, Suzuki E, Nishimatsu H, Satonaka H, Goto A, Omata M, Hirata Y. 2001. Transcriptional activation of the cyclin D1 gene is mediated by multiple cis-elements, including SP1 sites and a cAMP-responsive element in vascular endothelial cells. J Biol Chem 276:662–669.

Nakashima S, Matsuyama Y, Nitta A, Sakai Y, Ishiguro N. 2005. Highly efficient transfection of human marrow stromal cells by nucleofection. Transplant Proc 37:2290–2292.

Nishizawa M, Nagata S. 1992. cDNA clones encoding leucine-zipper proteins which interact with G-CSF gene promoter element 1-binding protein. FEBS Lett 299:36–38.

Ohtsubo M, Theodoras AM, Schumacher J, Roberts JM, Pagano M. 1995. Human cyclin E, a nuclear protein essential for the G1-to-S phase transition. Mol Cell Biol 15:2612–2624.

Pagano M, Pepperkok R, Verde F, Ansorge W, Draetta G. 1992. Cyclin A is required at two points in the human cell cycle. EMBO J 11:961–971.

Reddy TR, Tang H, Li X, Wong-Staal F. 1997. Functional interaction of the HTLV-1 transactivator Tax with activating transcription factor-4 (ATF4). Oncogene 14:2785–2792.

Roberts JM, Koff A, Polyak K, Firpo E, Collins S, Ohtsubo M, Massague J. 1994. Cyclins, Cdks, and cyclin kinase inhibitors. Cold Spring Harb Symp Quant Biol 59:31–38.

Roybal CN, Hunsaker LA, Barbash O, Vander Jagt DL, Abcouwer SF. 2005. The oxidative stressor arsenite activates vascular endothelial growth factor mRNA transcription by an ATF4-dependent mechanism. J Biol Chem 280: 20331–20339.

Sabbah M, Courilleau D, Mester J, Redeuilh G. 1999. Estrogen induction of the cyclin D1 promoter: Involvement of a cAMP response-like element. Proc Natl Acad Sci USA 96:11217–11222.

Sassone-Corsi P. 1994. Goals for signal transduction pathways: Linking up with transcriptional regulation. EMBO J 13:4717–4728.

Sherr CJ. 1994. G1 phase progression: Cycling on cue. Cell 79:551–555.

Sherr CJ, Roberts JM. 2004. Living with or without cyclins and cyclin-dependent kinases. Genes Dev 18:2699–2711.

Shi Y. 2002. Mechanisms of caspase activation and inhibition during apoptosis. Mol Cell 9:459–470.

Singha UK, Jiang Y, Yu S, Luo M, Lu Y, Zhang J, Xiao G. 2007. Rapamycin inhibits osteoblast proliferation and differentiation in MC3T3-E1 cells and primary mouse bone marrow stromal cells. J Cell Biochem 103:434–446.

Stacey DW. 2003. Cyclin D1 serves as a cell cycle regulatory switch in actively proliferating cells. Curr Opin Cell Biol 15:158–163.

Tanaka T, Tsujimura T, Takeda K, Sugihara A, Maekawa A, Terada N, Yoshida N, Akira S. 1998. Targeted disruption of ATF4 discloses its essential role in the formation of eye lens fibres. Genes Cells 3:801–810.

Tsujimoto A, Nyunoya H, Morita T, Sato T, Shimotohno K. 1991. Isolation of cDNAs for DNA-binding proteins which specifically bind to a tax-responsive enhancer element in the long terminal repeat of human T-cell leukemia virus type I. J Virol 65:1420–1426.

Vallejo M, Ron D, Miller CP, Habener JF. 1993. C/ATF, a member of the activating transcription factor family of DNA-binding proteins, dimerizes with CAAT/enhancer-binding proteins and directs their binding to cAMP response elements. Proc Natl Acad Sci USA 90:4679–4683.

Vinson CR, Hai T, Boyd SM. 1993. Dimerization specificity of the leucine zipper-containing bZIP motif on DNA binding: Prediction and rational design. Genes Dev 7:1047–1058.

Wang D, Christensen K, Chawla K, Xiao G, Krebsbach PH, Franceschi RT. 1999. Isolation and characterization of MC3T3-E1 preosteoblast subclones with distinct in vitro and in vivo differentiation/mineralization potential. J Bone Miner Res 14:893–903.

Wang J, Xi L, Hunt JL, Gooding W, Whiteside TL, Chen Z, Godfrey TE, Ferris RL. 2004. Expression pattern of chemokine receptor 6 (CCR6) and CCR7 in squamous cell carcinoma of the head and neck identifies a novel metastatic phenotype. Cancer Res 64:1861–1866.

Xiao G, Cui Y, Ducy P, Karsenty G, Franceschi RT. 1997. Ascorbic acid-dependent activation of the osteocalcin promoter in MC3T3-E1 preosteoblasts: Requirement for collagen matrix synthesis and the presence of an intact OSE2 sequence. Mol Endocrinol 11:1103–1113.

Xiao G, Jiang D, Gopalakrishnan R, Franceschi RT. 2002. Fibroblast growth factor 2 induction of the osteocalcin gene requires MAPK activity and phosphorylation of the osteoblast transcription factor, Cbfa1/Runx2. J Biol Chem 277:36181–36187.

Xiao G, Jiang D, Ge C, Zhao Z, Lai Y, Boules H, Phimphilai M, Yang X, Karsenty G, Franceschi RT. 2005. Cooperative interactions between activating transcription factor 4 and Runx2/Cbfa1 stimulate osteoblast-specific osteocalcin gene expression. J Biol Chem 280:30689–30696.

Yamanaka S, Tatsumi T, Shiraishi J, Mano A, Keira N, Matoba S, Asayama J, Fushiki S, Fliss H, Nakagawa M. 2003. Amlodipine inhibits doxorubicin-induced apoptosis in neonatal rat cardiac myocytes. J Am Coll Cardiol 41:870–878.

Yang X, Matsuda K, Bialek P, Jacquot S, Masuoka HC, Schinke T, Li L, Brancorsini S, Sassone-Corsi P, Townes TM, Hanauer A, Karsenty G. 2004. ATF4 is a substrate of RSK2 and an essential regulator of osteoblast biology; implication for Coffin-Lowry syndrome. Cell 117:387–398.

Yu VW, Ambartsoumian G, Verlinden L, Moir JM, Prud'homme J, Gauthier C, Roughley PJ, St-Arnaud R. 2005. FIAT represses ATF4-mediated transcription to regulate bone mass in transgenic mice. J Cell Biol 169:591–601.

Yu S, Franceschi RT, Luo M, Zhang X, Jiang D, Lai Y, Jiang Y, Zhang J, Xiao G. 2008a. Parathyroid hormone increases activating transcription factor 4 expression and activity in osteoblasts: Requirement for osteocalcin gene expression. Endocrinology 149:1960–1968.

Yu S, Jiang Y, Galson DL, Luo M, Lai Y, Lu Y, Ouyang HJ, Zhang J, Xiao G. 2008b. General transcription factor IIA-gamma increases osteoblast-specific osteocalcin gene expression via activating transcription factor 4 and runt-related transcription factor 2. J Biol Chem 283:5542–5553.

Zhao W, Byrne MH, Wang Y, Krane SM. 2000. Osteocyte and osteoblast apoptosis and excessive bone deposition accompany failure of collagenase cleavage of collagen. J Clin Invest 106:941–949.

Zhao J, Pestell R, Guan JL. 2001. Transcriptional activation of cyclin D1 promoter by FAK contributes to cell cycle progression. Mol Biol Cell 12: 4066–4077.

Zhao M, Qiao M, Harris SE, Oyajobi BO, Mundy GR, Chen D. 2004. Smurf1 inhibits osteoblast differentiation and bone formation in vitro and in vivo. J Biol Chem 279:12854–12859.

Ziff EB. 1990. Transcription factors: A new family gathers at the cAMP response site. Trends Genet 6:69–72.